Front. Mater. Sci. 2012, 6(1): 26–46
DOI 10.1007/s11706-012-0160-x

REVIEW ARTICLE

Carbon nanomaterials: controlled growth and field-effect transistor biosensors

Xiao-Na WANG[1,2] and Ping-An HU (✉)[1,2]

1 Key Laboratory of Micro-systems and Micro-structures Manufacturing (Ministry of Education), Harbin Institute of Technology, Harbin 150080, China
2 Micro/Nano Technology Research Center, Harbin Institute of Technology, Harbin 150080, China

ABSTRACT: Carbon nanostructures, including carbon nanotubes (CNTs) and graphene, have been studied extensively due to their special structures, excellent electrical properties and high chemical stability. With the development of nanotechnology and nanoscience, various methods have been developed to synthesize CNTs/graphene and to assemble them into microelectronic/sensor devices. In this review, we mainly demonstrate the latest progress in synthesis of CNTs and graphene and their applications in field-effect transistors (FETs) for biological sensors.

KEYWORDS: carbon nanotube (CNT), graphene, preparation, field-effect transistor (FET), biosensor

Outline

Received January 4, 2012; accepted February 5, 2012

E-mail: hupa@hit.edu.cn

1 Introduction

Carbon (from Latin: *carbo* “coal”) is the unique chemical element with strong capability to form long chain with its own atoms. The strong and stable carbon–carbon bonds render production of an enormous number of molecular forms. Up to date, over ten million carbon containing compounds are known and many of them are important structural elements of life. Classical allotropes of carbon existing in nature are known to be graphite, diamond, and amorphous carbon for a few thousand years. In past thirty years, several new allotropes of carbon have been discovered: Fullerene, which is a molecule containing 60 carbon atoms in the soccer-ball-shape, was discovered in 1985 [1]; Six years later, carbon nanotube (CNT), a tubular-macromolecule, was reported by Iijima [2], a Japanese

scientist; Graphene, a single atomic layer of graphite, was discovered in 2004 by two scientists [3], who were therefore both awarded the Nobel Prize in Physics for the year 2010.

Among those allotropes of carbon, CNTs and graphene are of importance to modern science and technology since they provide exciting challenges and opportunities for chemists, physicists, biologists and materials scientists. Their growing interests are evidenced by increasing number of relevant publications from 1995 to 2011 (shown in Fig. 1). In this period, the number of publications of CNTs is tremendously larger compared to that of graphene. However, publication of CNTs shows a little decrease in 2010 than that in 2011, which reflect the research situation of CNTs field since they have been studied for twenty years; Publication number of graphene rise tremendously from 2004 to 2011, indicating that graphene is an infant and star field. It is expected that more and more scientists will follow with interest in graphene in near future. Anyway, this statistics of publications reveal that CNTs and graphene play a special role in nanotechnology. Preparation and application in electrical and biosensors are both central to the research field of CNTs and graphene. Herein, we review the latest progress in the preparation, assembly and biosensor of CNTs and graphene and provide prospect for the future development.

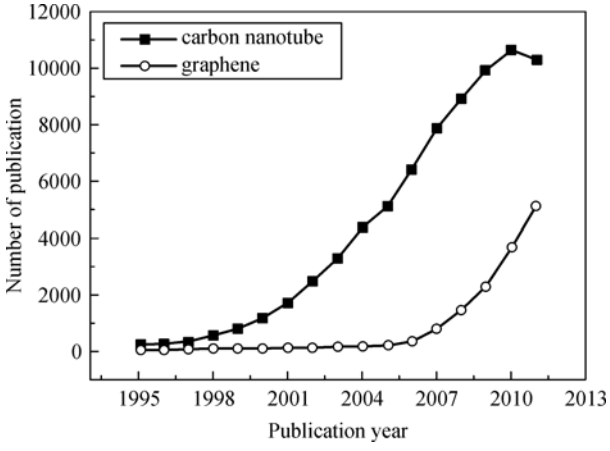

Fig. 1 Statistics of papers published year by year relevant to CNT and graphene. Data analysis is based on Web of Knowledge as of December 2011.

2 CNTs

CNTs are one of the advanced functional materials and have been researched extensively since it was first reported in *Nature* in 1991 by Iijima [2]. CNTs belong to a family of quasi one-dimensional tubular structures, which can form by rolling up graphene sheet(s) made up of single layer of sp^2 carbon atoms that are densely packed in a honeycomb lattice structure. Depending on the layer number of graphene sheets, single-walled carbon nanotubes (SWNTs) can be obtained. SWNTs have attracted the widespread attention because of their excellent electrical (carrier mobility as high as 100,000 $cm^2 \cdot V^{-1} \cdot s^{-1}$), mechanical (Young's modulus of 1 TPa and tensile strength of 30 GPa), thermal (6600 $W \cdot m^{-1} \cdot K^{-1}$ at room temperature), optical and sensing properties [4]. All these excellent properties make SWNTs wide potential applications in the field of nano-electronic devices, optoelectronic devices, nanosensors, transparent and conducting membranes and composites [5–13]. These applications require controlled growth or assembly of CNTs which pose characteristics of defined locations, desired directions or controlled density.

2.1 Controlled growth of CNTs

CNTs can be prepared by main approaches including chemical vapor deposition (CVD) [14–15], arc discharge [16–17] and laser ablation [18]. In recent years, most of studies regarding CNT production are mainly on the controlled growth of CNTs with functional structure including intramolecular junction nanotubes and aligned nanotubes.

2.1.1 Intramolecular junctions of CNTs

The basic building elements in microelectronics are various junctions such as P-N junction, Shottky junctions, etc. Therefore, intramolecular junctions of CNTs are expected to have fascinating applications in future nanodevices. SWNT/SWNT junctions can be frequently observed in normal SWNT samples produced by a CVD process [19], laser ablation method [20], and arc discharge method [21]. However, they only grew inadvertently in most cases. Cubukcu et al. found that the introduction of sulfur containing precursors such as thiophene into the CVD process could largely promote the formation of SWNT/SWNT junctions, as sulfur could change the active site on the catalyst, which caused a change of the CNT growth direction to form SWNT/SWNT junctions formed [22]. Recently, Yao et al. reported a well-controlled synthesis of the SWNT/SWNT junctions by a temperature-mediated CVD method [23]. This method is based on the temperature effect on the diameter of the growing nanotube, such that a higher temperature leads to thinner SWNTs with the same catalyst particle, and vice versa. If

the temperature changes in the growth, an intramolecular junction would form along the SWNTs. If the temperature changes several times during the growth, sequential intramolecular junctions would form along the SWNTs.

Doping substitution of carbon atoms with other elemental atoms including nitrogen, boron in the CNT is an efficient way to grow intomolecular junction nanotube. The general route for synthesis is by a two-step CVD process, in which pristine CNTs grow in the first step, and then the junctions form when doped CNTs continuously grow from the pristine CNTs by introducing dopant precursor in the second step. For instance, Hu et al. has reported controllable synthesis of CN_x/C nanotubes with intramolecular junctions by adjustable inlet of ammonia gas [24]. The nanotubes consist of two sections, one section made of carbon nitride featuring bamboo-like structure and the other one made of carbon featuring empty hollow cylinder structure, and thus the intramolecular junctions were formed in the middle as a result of being doped or undoped with nitrogen (Fig. 2). The CN_x/C intramolecular junctions show typical rectifying diode behavior by measuring *I*–*V* characteristics with a rectification ratio of 1.3×10^3 at $\pm$ 2 V. The nanodiode demonstrated as a half-wave rectifier worked at an input sine wave of 1 kHz. On the other hand, the intramolecular junctions could be interconnected as diode logic OR and AND gates by two CN_x/C junctions configured together. More important, after substituting the wave-detection silicon diode in common transistor radio set with our nanodiode, the radio set still worked normally, representing an important step toward the potential application for nanoscale devices. Recently Wei et al. demonstrated a flow fluctuation CVD method to efficiently produce branched CNTs with multiple junctions [25–26] and a high yield (above 90%) was achieved. The branched junctions had a similar configuration in that two or more branches with similar diameters, which were oriented in nearly the same direction, converged into a larger diameter stem.

2.1.2 Growth of aligned SWNTs

Growth of aligned SWNTs parallel to substrate is essential for the integration of nanotube based nanoelectronics. In addition, one-dimensional structure of SWNTs has anisotropic mechanical, electric and optical properties. Generally, most of their properties along the tube axis are better than that perpendicular to the tube axis orientation. Therefore, the alignment of CNTs with controlled position and orientation is highly in need.

Conventional CVD process on flat substrates usually produces randomly oriented SWNTs, probably because the strong van der Waals interaction between catalyst nanoparticles and substrate may hinder the alignment of SWNTs during growth and even poison the catalyst [27]. Several studies have demonstrate that growth of SWNTs by CVD on crystalline substrates such as sapphire and quartz can

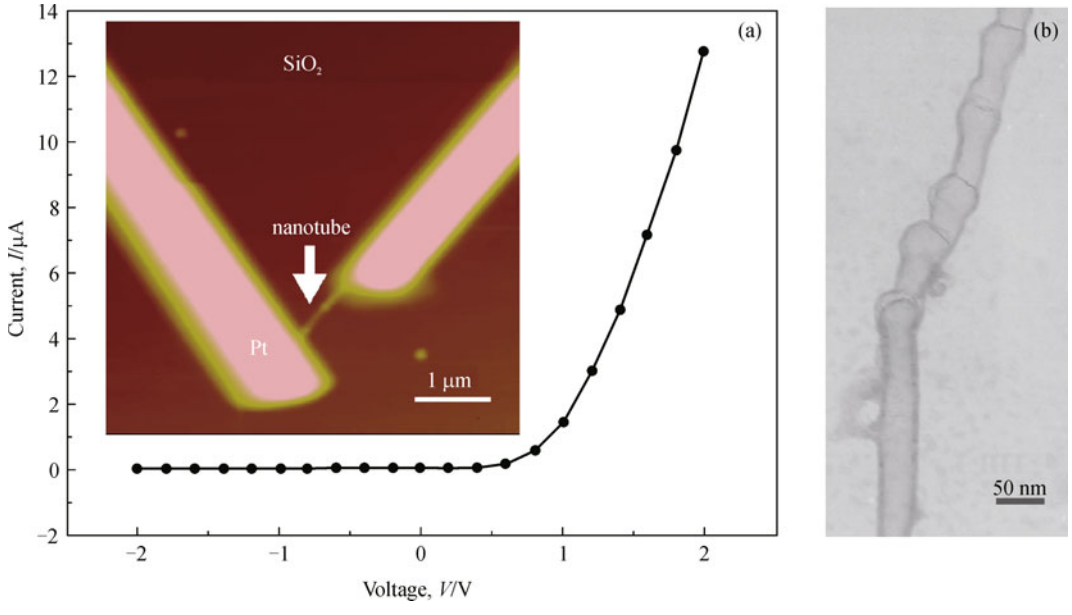

Fig. 2 **(a)** Current–voltage characteristics of a CN_x/C nanotube measured at room temperature showing rectifying behavior. Inset: contacting-mode atomic force microscope image of an example of a nanotube junction device with Pt contacts. **(b)** Individual C/CN_x nanotube. (Reproduced with permission from Ref. [24], Copyright 2004 American Institute of Physics)

produce nearly ideal arrangements of pristine, low-defect tubes, which are probably caused by surface interactions between SWNTs and single crystal substrates with anisotropic lattices or miscut atomic steps. The best results have been reported on quartz, where levels of alignment can be controlled to better than 0.01, with linear shapes to within a few nanometers over lengths of many micrometers, in tubes with average lengths of hundreds of micrometers (up to ~ millimeters). For instance, Ding et al. [28] demonstrated preparation of high-density and perfectly aligned arrays of semiconducting SWNTs on stable temperature (ST)-cut quartz substrates using copper as catalyst and ethanol as carbon source (shown in Fig. 3). A patterned catalyst is used for the growth of long and straight nanotubes with high density. The length of the nanotubes can be controlled by the spacing between catalyst patterns, and the diameter has an intrinsically narrow distribution around 1.2 nm. The density can reach $>$ 50 nanotubes per micron and the length can be a few millimeters. Ishigami et al. have reported that not only the orientation, but also the diameter and chirality of SWNTs are affected by the crystal plane of the sapphire substrate [29]; The aligned SWNTs grown on the A- and R-planes of sapphire had narrower diameter distributions than randomly oriented tubes produced on the C-plane sapphire and amorphous SiO_2. Photoluminescence measurements revealed a striking difference between the aligned SWNTs: near-zigzag tubes were observed on the A-plane and near-armchair tubes on the R-plane. This study showed the route for the diameter and chirality control of SWNTs by surface atomic arrangements of a single-crystal substrate.

Gas flow CVD is another efficient way to synthesize highly oriented SWNTs. As shown in Fig. 4, Jin et al. reported growth of horizontally aligned ultralong SWNT arrays without the use of any other external driving force or special substrates by using ultralow gas flow [30]. High-quality SWNT arrays along the gas flow direction can be grown with several sccm (standard cubic centimeter per minute) of feeding gas. By mounting small tubes containing silicon wafers side-by-side into the quartz tube of the CVD system, batch scale preparation was achieved under low gas feeding flow rate. From the experiments of SWNT arrays growing across microtrenches and micro-obstacles as well as on silicon substrates with different obliquities, it was deduced that, in the ultralow flow rate process, the growing SWNTs can still be lifted up from the substrates and navigated by the gas flow. They also found that the temperature/density gradient induced buoyancy effect plays an important role, and the steady and highly laminar gas flow is very suitable for piloting the growth of paralleled long tubes. Liu and co-workers also developed a "fast heating" CVD technique to achieve the growth of long and aligned SWNTs on silica/silicon surfaces. This method can also be used to directly grow two-dimensional crossed network of SWNTs by a two-step growth process. In subsequent work, they proposed a "kite mechanism" to explain the growth of aligned SWNTs by "fast heating" CVD process [31]. The laminar flow-assisted technique is another successful strategy for the growth of aligned CNTs. It is accepted that a stable laminar gas flow, which facilitate to stabilize the catalysts at the end of growing CNTs and make the catalysts travel long distances, plays a key role in the growth of long and aligned CNTs [32]. The stability of the gas can be estimated by the Reynolds number $Re = qmd/c$, where q is the density of gas mixture, m is the flow speed, d is the furnace tube diameter, and c is gas coefficient viscosity. To grow aligned CNTs, the flow should be controlled as laminar flow ($Re < 2000$). When $Re > 2000$, the flow is unstable turbulent flow and can not support the growth of aligned CNTs.

2.2 SWNT-FET biosensors

Label-free biosensors with high miniaturization and integration have drawn intense research interest since they could potentially make advanced molecular diagnostics available for low cost routine practice. Current sensing mainly focuses on optical detection, using fluorescent-labeled biomolecules with dyes [33–35] or quantum dots [36–38]. The artificial labeling of materials is time-consuming and cost-intensive, and introduction of labels can weaken the interaction between receptor and target. Hence, the development of fully electronic and label-free sensing techniques is required. The electrical conductance of a semiconducting SWNT is sensitive to its environment and varies significantly with surface adsorption of various chemicals and biomolecules [39–41]. This makes SWNT based field-effect transistors (FETs) very promising candidates for label-free biosensing. As shown in Fig. 5, SWNT-FET biosensors are composed of SWNT networks or individual semiconducting SWNTs which lie on SiO_2/Si wafer and two metallic source/drain electrodes. To allow for identification of such biological interactions through electrical monitoring, the transfer characteristics of SWNT-FET can be measured using an electrolyte as a top gate or the Si substrate as a back gate. For the back gate transfer

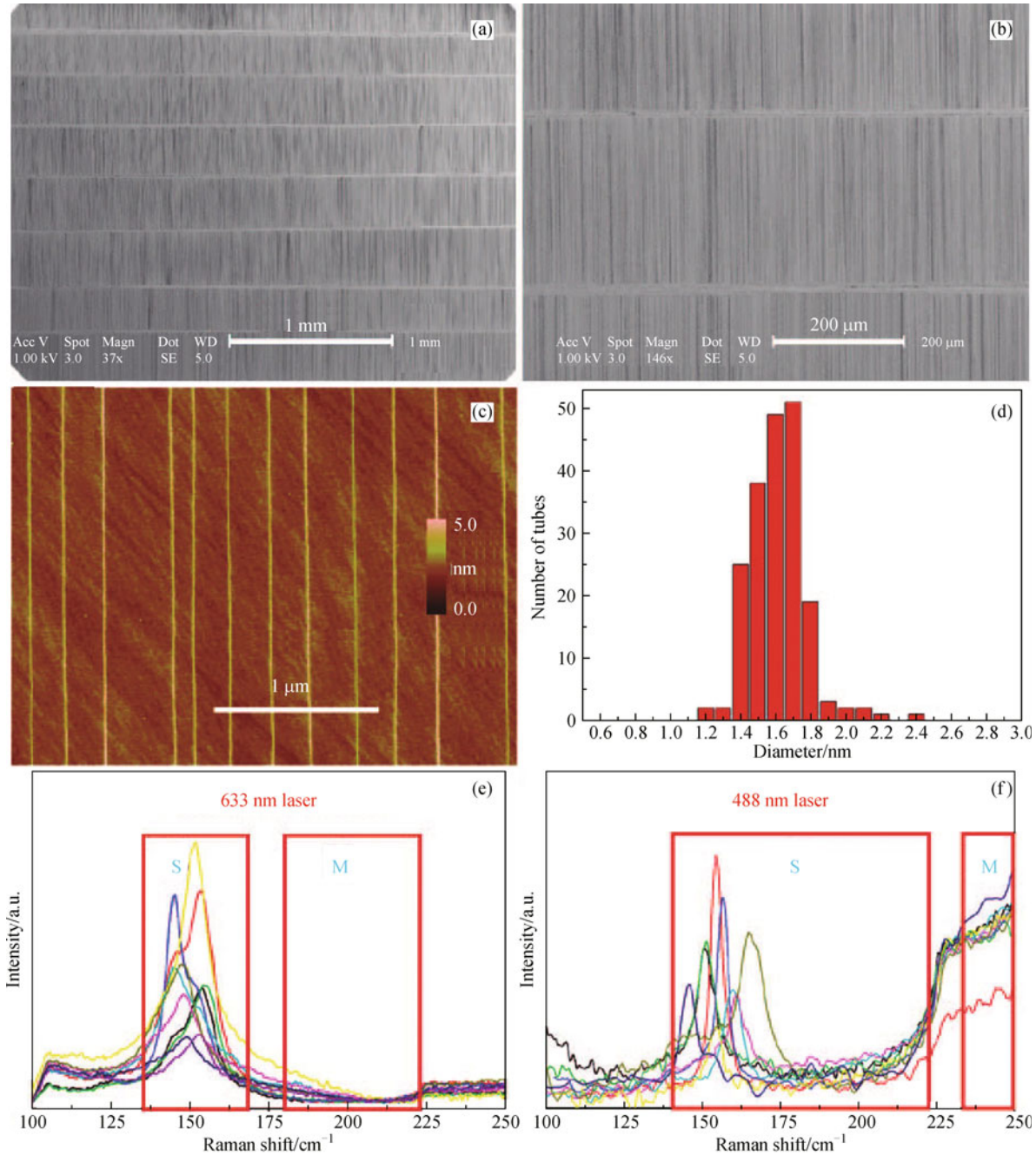

Fig. 3 Arrays of almost exclusively semiconducting SWNTs. **(a)(b)** SEM images. The bright and parallel horizontal lines visible in the images are catalyst lines. **(c)** AFM image. **(d)** Diameter distribution of 200 SWNTs of an array measured by AFM. **(e)(f)** Raman spectra of SWNTs transferred onto the SiO_x/Si substrates. The spectra were obtained using 488 and 633 nm excitation laser lines at 10 different spots over the substrate for each laser line. Each curve in a panel shows a spectrum at a spot on the substrate. Peaks within the rectangles marked with S correspond to the semiconducting SWNTs. The rectangles marked with M denote the frequency range where RBM peaks of metallic SWNTs are expected. (Reproduced with permission from Ref. [28], Copyright 2009 American Chemical Society)

characteristics, the current through the drain contact (at fixed drain-source bias) is measured while a variable gate voltage is applied through a back gate buried underneath the SiO_2 substrate. The electrolyte top gate transfer characteristics are concerned, the device is immersed in a buffer solution and a variable gate voltage is applied through an external electrode immersed in the electrolyte, while the drain current is monitored. SWNT-FET based biosensors have been reported to detect various biological species such as DNA, protein and cells.

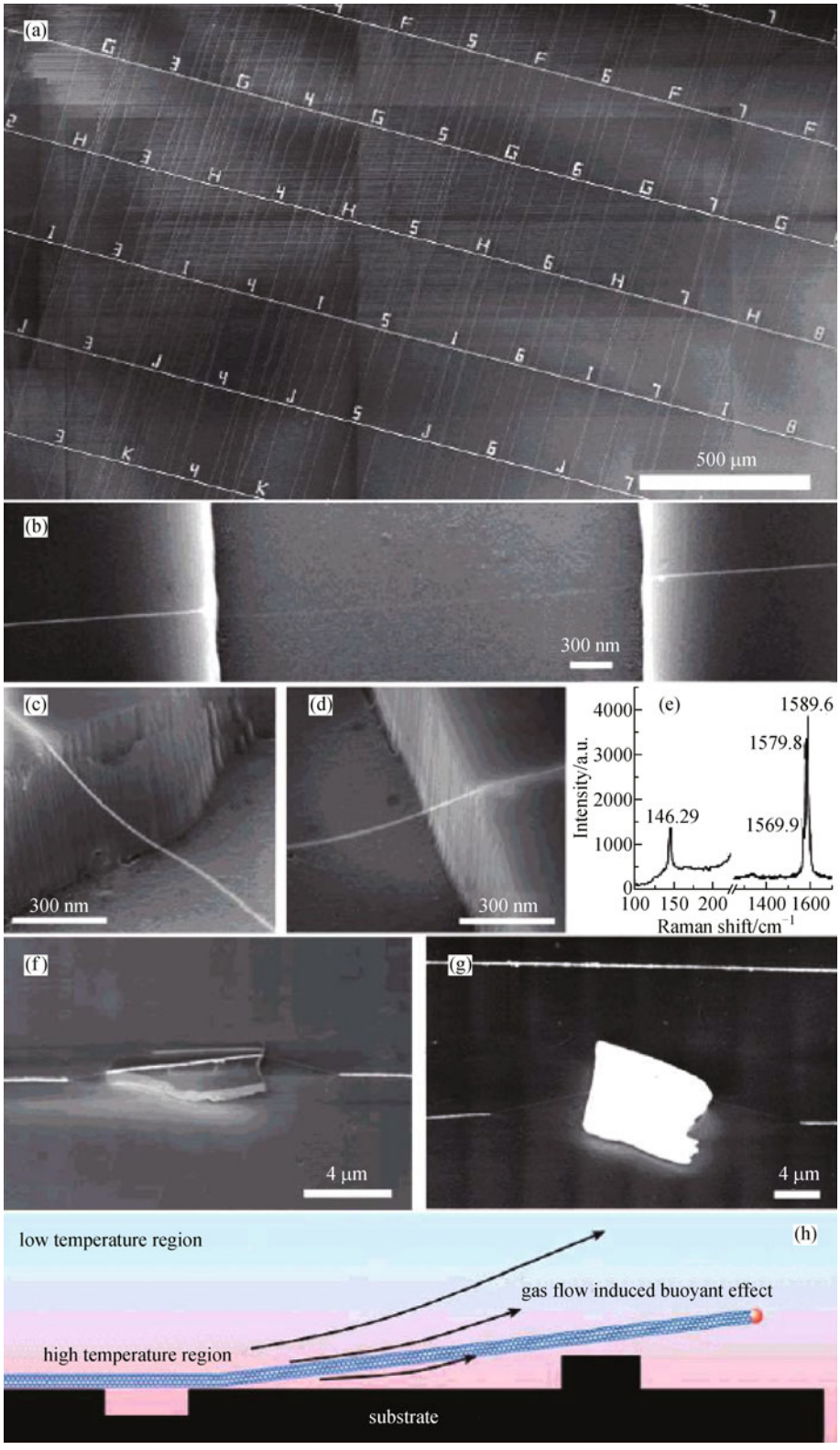

Fig. 4 **(a)** SEM image of SWNT arrays grown across microtrenches. **(b)** A suspended SWNT crossing over a microtrench, the two ends of this SWNT "rope bridge" are shown in **(c)** and **(d)**, respectively. **(e)** Raman spectrum measured from the center part of the suspended SWNT. **(f)(g)** SEM images of SWNTs grown over micro-obstacles. **(h)** Schematic drawing of the growth mechanism. The front section of a growing SWNT floats in low rate gas flow relying on the buoyant effect induced by gas density/temperature gradient (shown as the gradual change of background color) and shear flow near the substrate surface. (Reproduced with permission from Ref. [30], Copyright 2007 American Chemical Society)

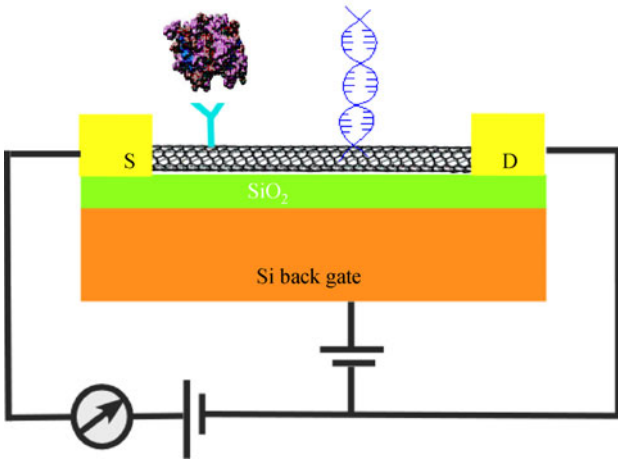

Fig. 5 Schematic drawing of SWNT-FET biosensors.

2.2.1 SWNT-FET based DNA sensors

SWNT-FET sensors which measure DNA hybridization hold great potential for wide scale of genetic testing, clinical diagnostic and fast detection of biological warfare agents. Much attention has been given to the problem of interaction of CNTs and DNA with the purpose for the application in drug delivery and sensing. Nucleic acids including single-stranded DNA (ssDNA) and RNA can disperse SWNTs in water. Interaction of DNA and SWNT in water is due to nucleic acid base π-stacking on the nanotube surface, resulting on the hydrophilic molecular part pointing to the outside. ssDNA has been demonstrated to interact non-covalently with SWNTs [42–43] and form a stable hybrid with individual SWNTs by wrapping around them by means of the aromatic interactions between nucleotide bases and SWNT sidewalls. Molecular modeling suggests that ssDNA can bind to CNTs through π-stacking, resulting in helical wrapping to the surface (Fig. 6(a)). This interaction is dependent on the DNA sequence, which is used for structural separation of SWNTs. In addition, theoretical research shows that double-stranded DNA (dsDNA) molecules can interact with SWNTs as major groove binders.

The promising application of functionalized SWNTs in monitoring DNA hybridization was demonstrated by Dekker et al. in 2002 [44]. A coupling peptide nucleic acid (PNA) – an uncharged DNA analogue – was covalently linked to the carboxyl-functionalized tip of SWNTs. Then PNA-DNA hybridization was measured by using atomic force microscopy (AFM). This work laid the foundation for the subsequent development of SWNTs based biosensors. Star et al. reported SWNT network FETs that function as selective detectors of DNA immobilization and hybridization [45]. As shown in Figs. 6(b) and 6(c), SWNT network FETs with immobilized synthetic oligonucleotides have been shown to specifically recognize target DNA sequences via electrical response; DNA hybridization with complementary target DNA sequences resulted in reduction of the SWNT-FET conductance. The sensing mechanism relies on the fact that ssDNA adsorbed on sidewalls of SWNTs can result in electron doping to the SWNT semiconductor channels. This SWNT-FET DNA sensor can detect samples with picomolar to micromolar DNA concentrations. Gui et al. reported that SWNT-FET immobilized with ssDNA oligomers encoded with a terminal NH_2 (NH_2-DNA) show reliable detection and differentiation of its complementary and single-base mismatched DNA strand [46]. The sensitivity was further enhanced by using threading intercalators. Sensing mechanism of electrical detection of DNA for this network SWNT-FET was further investigated, showing that sensing of DNA is dominated by the variety in metal-SWNT junctions rather than the channel conductance [47]. Dong et al. demonstrated the sensitivity of a network SWNT DNA sensor to be enhanced by employing gold nanoparticle (AuNP) linked DNA target hybrid – DNA detection was observed for concentrations at the femtomolar level [48]. Very recently, Tseng and coworkers have developed a new approach to ensure specific adsorption of DNA to the nanotubes [49]. A polymer was bonded covalently to nanotube in an FET consisting of individual SWNTs. After hybridization, statistically significant changes were observed in key transistor parameters. Hybridized DNA traps both electrons and holes, possibly caused by the charge-trapping nature of the base pairs. Tao et al. reported the unambiguous detection of a sequence of Hepatitis C Virus (HCV) at concentrations down to the fractional picomolar range using SWNT-FET devices functionalized with peptide nucleic acid sequences [50].

2.2.2 SWNT-FET based protein sensors

A great deal of research towards biosensing involves proteins and CNTs. Proteins can strongly bind to the nanotube surface via nonspecific binding (NSB). This NSB interaction is proposed to be in part associated with the amino affinity of CNTs according to recent research [51–52]. Two generalized approaches for this modification of SWNTs are covalent or non-covalent functionalization. As for covalent methods, the SWNTs are usually oxidized to

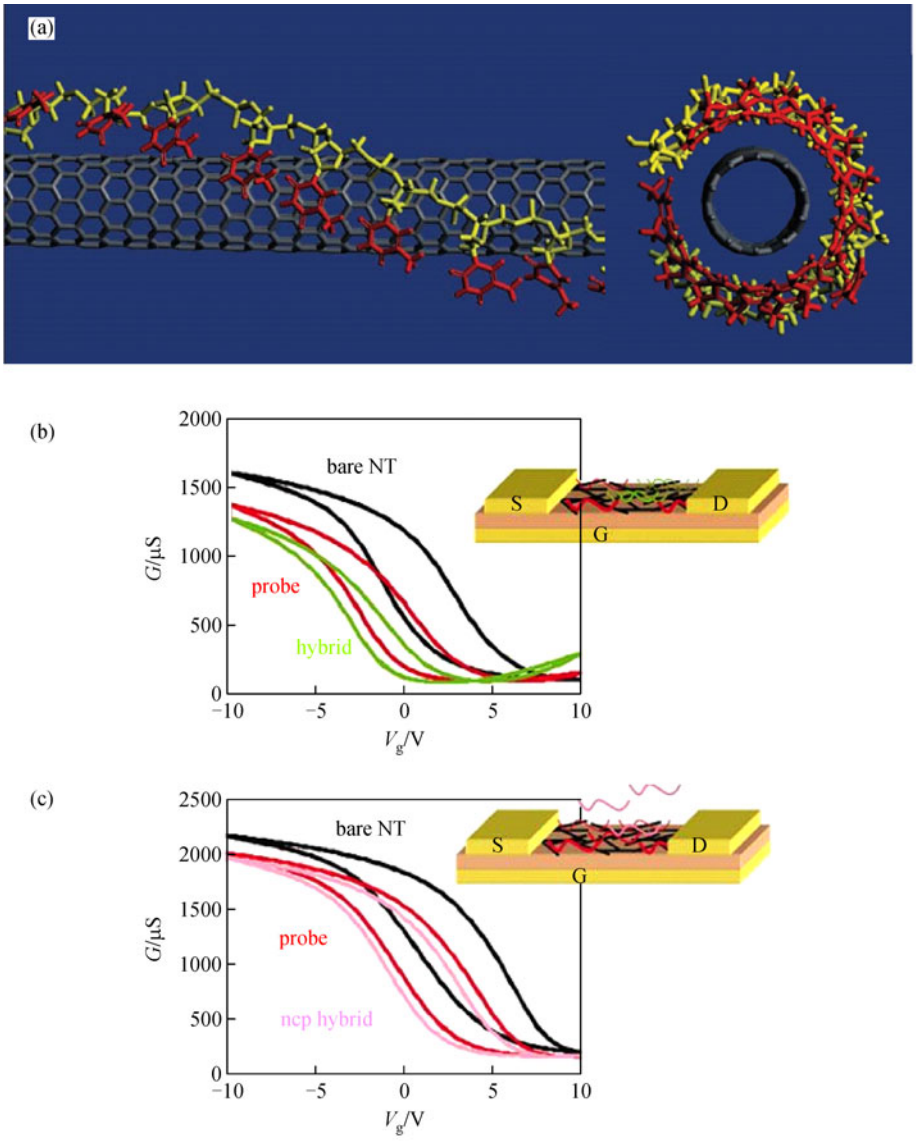

Fig. 6 **(a)** Aromatic nucleotide bases in the ssDNA are exposed to form π-stacking with the sidewall of the SWNT. (Reproduced with permission from Ref. [43], Copyright 2003 Nature Publishing Group) Electronic measurements such as source-drain conductance (G) as function of gate voltage (V_g), and schematic drawings of the NTNFET devices used for DNA assays: **(b)** Before (bare NT) and after incubation with 12-mer oligonucleotide capture probes (5′-CCT AAT AAC AAT-3′), as well as after incubation with the complementary FITC-labeled DNA targets; **(c)** Before and after incubation with dA_{12} captures as well as after incubation with the DNA targets. (Reproduced with permission from Ref. [45], Copyright 2006 The National Academy of Sciences of the United States of America)

produce free carboxyl groups for coupling with amino groups in proteins. These occur predominantly at tips or defects in SWNTs. The protein is then covalently linked to the carboxyl functionalized SWNTs using standard N-hydroxysuccimide/carbodiimide chemistry [53]. In addition, sidewall modification of SWNTs can be performed by using nitrene, clycloaddition, arylation in the presence of a diazonium salt or 1, 3-dipolar cycloaddition [54]. Although covalent modification is effective at introducing functionality, it often destroys the desirable mechanical and electrical properties of the SWNTs. On the other hand, the non-covalent approach exploits nondestructive processes and can preserve the primary structures and the unique properties of SWNTs. In term of the non-covalent procedure, certain molecules which act as linkers for biomolecules are first non-covalently coated onto SWNTs, and biomolecules are then covalently bound to the linkers. Dai's group first demonstrated a two-step hybrid modification of SWNT with

proteins [55]: 1-pyrenebutanoic acid, succinimidyl ester was first irreversibly adsorbed onto an SWNT via π-stacking interaction; proteins were then immobilized through a nucleophilic substitution of N-hydroxysuccinimide by an amino group on the proteins that forms an amide bond. Furthermore, they suggested a strategy to the solve NSB problems. This NSB suppression strategy involves non-covalently coating SWNTs with polyethylene glycol (PEG) containing polymers such as Tween 20. The PEG coating renders the SWNT highly hydrophilic and charge-neutral, thereby eliminating hydrophobic interaction and electrostatic binding with proteins [56].

The conductance of SWNTs shows sensitive response to a variety of chemical or biological environments. Therefore, biological recognition – such as antibody-antigen interactions – occurring at an SWNT surface can be monitored by electrical measurement of an FET device. The first demonstration of a CNT-FET protein biosensor was reported by Dekker et al. [57]. The device was made of individual SWNTs and a variable electrolyte gate voltage was applied through a platinum electrode. The enzyme glucose oxidase (GOx) that catalyzes the oxidation of glucose to glucono-1, 5-lactone, was non-covalently coupled to the sidewall of the SWNTs via a linker molecule of 1-pyrenebutanoic acid succinimidyl ester. The observed decrease in conductance is attributed to the change in the capacitance of the nanotube caused by GOx immobilization. An estimated 50 molecules of GOx were immobilized over the nanotube length of 600 nm. The enzyme layer on the SWNT can inhibit ions in the liquid to come close to the nanotube, thereby decreasing the double layer capacitance and hence the capacitance of the nanotube. However, the possibility of charge scattering at the SWNT in the presence of the GOx molecules cannot be ruled out completely. Dekker et al. further demonstrated a strong pH-dependent conductance of the GOx immobilized SWNT, which is presumably due to the pH sensitivity of the charged groups on the GOx molecules, which become more negative with increasing pH. The GOx-SWNT system exhibited real time sensing of glucose, thus rendering such a nanoscale FET device as a feasible sensor for monitoring enzymatic activity at single-molecule level. Dai et al. reported a general non-covalent approach for the configuration of CNT protein biosensors [41]. Polymers such as Tween 20 or triblock copolymer chains, which are irreversibly adsorbed on nanotubes, act as linkers for binding the biomolecules of interest and as the inhibitor for NSB of proteins. The as-fabricated CNT sensors exhibited selective recognition and binding of target proteins by conjugation of their specific receptors to polyethylene oxide-functionalized nanotubes. In particular, they have studied the affinity binding of 10E3 mAbs antibody (a prototype target of the autoimmune response in patients with systematic lupus erythematosus and mixed connective tissue disease) to human auto antigen U1A. Hu et al. observed a reverse change in the electrical monitoring of biotin-streptavidin interaction using SWNT-FETs [58]. A large area SWNT-FET was fabricated by a self-assembled method whereby the electrode surface and the area between electrodes were modified with nonpolar groups (CH_3) or polar groups (NH_3^+). The SWNTs were selectively placed in the area between the electrodes (Fig. 7). The drain-source current at a fixed gate voltage showed an obvious increase upon the binding of streptavidin onto the biotin functionalized SWNT-FET. This increase in conductance upon addition of streptavidin is consistent with binding of negatively charged species to the surface of a p-type SWNT since streptavidin (with an isoelectronic point pI between 5 and 6) is negatively charged at the pH of the measurements (pH 7.2). The sensing mechanism is consistent with electrolyte gating rather than charge transfer as in the work of Star et al. [45]. Furthermore, Hu et al. studied the specificity and real-time detection of the as fabricated CNT-FET biosensor by using bovine immunoglobulin G (IgG) as a control protein [58].

2.2.3 Sensing mechanism of SWNT-FET biosensors

CNT biosensors have a variety of advantages over conventional chemical and biological sensors due to large surface to volume ratios resulting in higher sensitivity, potential for miniaturization and lower power consumption. In order for CNT sensors to replace conventional sensors, some issues such as the sensing mechanism should be resolved. The physical mechanism underlying sensing is still under debate due to very different conductance effects observed upon sensing, and due to the different interpretations given to similar conductance variations. Star et al. reported a decrease in conductance upon the biotin-streptavidin interaction on SWNT-FETs and attributed this change to charge transfer [59], while Hu et al. observed the reverse conductance effect from the biotin-streptavidin interaction on SWNT-FET and explained this phenomenon by electrolyte gating [58]. In addition, the observed decrease in transconductance during protein sensing by

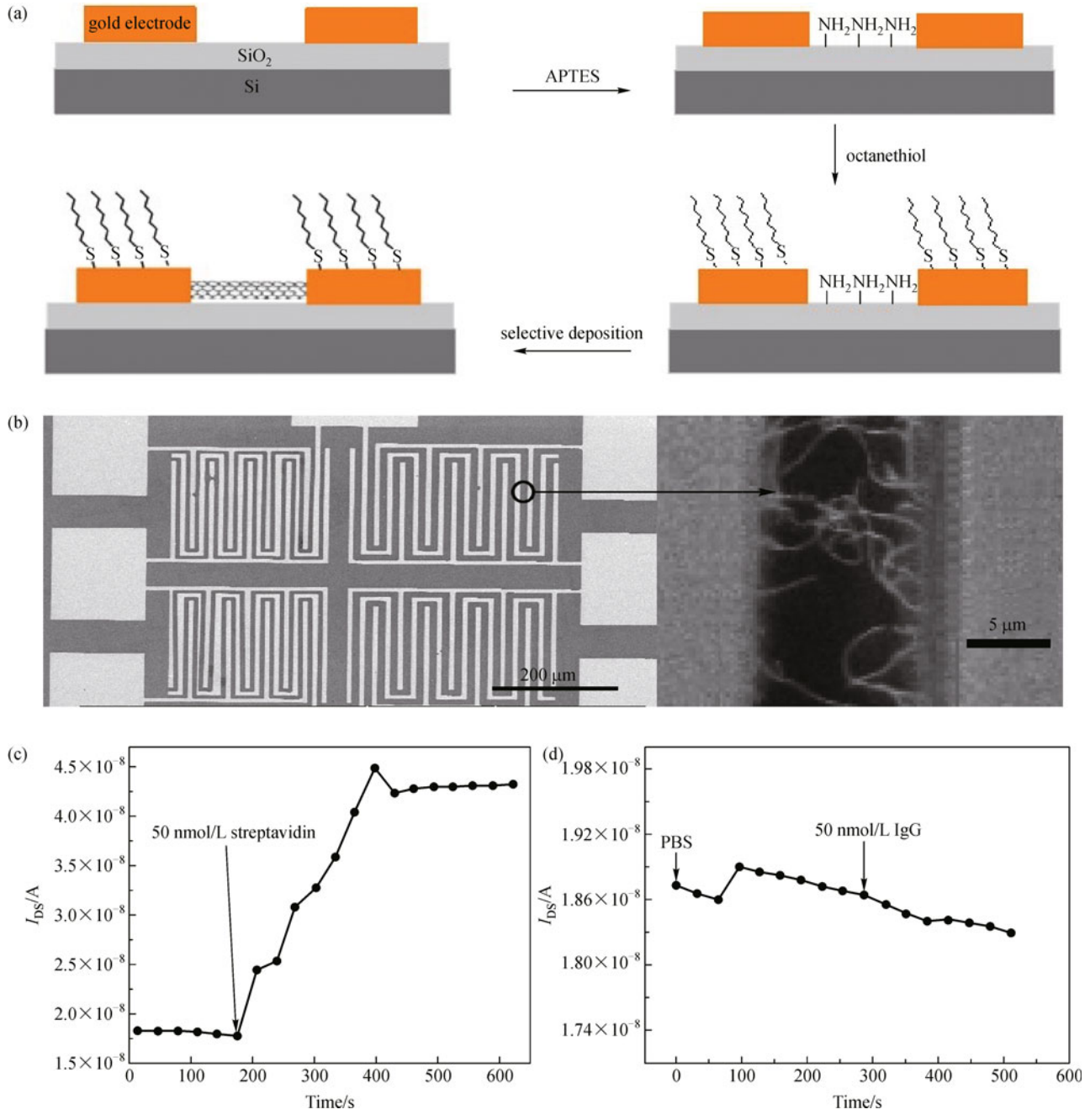

Fig. 7 **(a)** Scheme of the self-assembly procedure for SWNT-FET fabrication. **(b)** SEM images of FET chip; magnified images show SWNTs selectively deposited between electrodes, contacting source and drain. Note that the electrode surface is shown to be clean. **(c)** Real time analysis: time dependence of I_{DS} at V_{DS} = 0.2 V and at V_{GS} = –5 V upon the introduction of target streptavidin (50 nmol/L) onto the biotinylated device. Adding the target streptavidin causes a sharp increase in the source-drain current and then a gradual saturation at slightly lower values. **(d)** No effect is observed upon the addition of IgG. (Reproduced with permission from Ref. [58], Copyright 2008 American Institute of Physics)

SWNT-FETs cannot be attributed totally to the scattering of mobile charges. There is the possibility of change in the Schottky barrier (SB) height at the contact of metal-nanotube, which can modulate the conductance of the device. So far, four proposed possible mechanisms that account for the variety in conductance effects of SWNT-FET biosensors are electrostatic gating, capacitance modulation, SB effects and carrier mobility change [60–66]. Recently, through modeling and protein adsorption experiments, Dekker et al. further studied the mechanisms of biosensing with SWNT-FETs [67]. They discovered that electrostatic gating and SB effects are two relevant

mechanisms, while electrogating is most reproducible. In particular, the sensing is dominated to be electrostatic gating if the metal electrodes are passivated.

3 Preparation and biosensor of graphene

Graphene, a flat monolayer of carbon atoms packed into a two-dimensional honeycomb lattice, has become one of most interesting topic of research since its discovery in 2004 [3]. It can be seen as the basis of all carbon materials including fullerenes and CNTs [68]. Graphene can be wrapped to form fullerene, scrolled to form a CNT and stacked to form graphite (Fig. 8). Graphene has a large theoretical specific surface area ($2630\ m^2 \cdot g^{-1}$), high intrinsic mobility ($200{,}000\ cm^2 \cdot V^{-1} \cdot s^{-1}$) [2–3], high Young's modulus (1.0 TPa), thermal conductivity ($5000\ W \cdot m^{-1} \cdot K^{-1}$) and its optical transmittance (97.7%), and good electrical conductivity merit attention for applications such as for transparent conductive electrodes and many other potential applications.

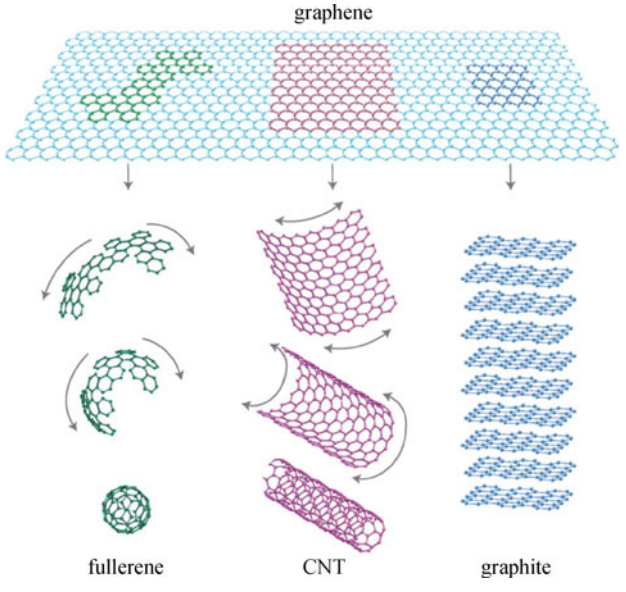

Fig. 8 Graphene and its relation to fullerene, CNT and graphite. (Reproduced with permission from Ref. [68], Copyright 2007 Nature Publishing Group)

3.1 Preparation of graphene

Preparation is one of central research aspects in graphene field. The best quality graphene, in terms of structural integrity, is produced by mechanical cleavage of highly oriented pyrolytic graphite (HOPG). Mechanically cleaved graphenes have very low concentration of structural defects, which makes them interesting for fundamental studies. However, this approach produced the graphene flakes with uncontrolled thickness, size and location. Therefore, several strategies are presently pursued to achieve reproducible and scalable graphenes, which includes epitaxial techniques [69–71], chemical exfoliation, CVD and other novel approaches. The explicit introductions of these approaches are given below.

3.1.1 Epitaxial growth

The typical example of epitaxial growth is conversion of SiC(0001) to graphene via sublimation of silicon atoms at high temperatures [70]. High quality wafer scale graphene with switching speeds of up to 100 GHz has been demonstrated using this technique. Although the price of the initial SiC wafer is relatively high compared to that of silicon, the technique maybe suitable for radio and THz frequency electronics where the excellent performance of the devices could offset the cost of the wafers.

3.1.2 Chemical exfoliation

Reduced graphene oxide (rGO) produced from chemical or thermal reduction of graphene oxide (GO) is competitively alternative material of graphene. GO prepared from graphites via chemical exfoliation method emerges as single-layer graphene (SG) or few-layer graphene (FG) with high yield production dispersions (~4 mg/mL). The solution processability of GO offers unique advantages since it is readily amenable for spin-coating, casting, transferring, imprinting onto substrates for large-scale production of graphene electronic circuits. Especially, residual chemically active defect sites render rGO a promising material for functional electronic sensors. Some chemical/biological sensors made from single-layer rGO or few-layer rGO have been demonstrated [71–74]. Preparation of graphite oxide can be achieved by treatment of graphite in one or more concentrated acids with an oxidizing agent. Graphite oxide was first prepared by Brodie, who treated graphite repeatedly with potassium chlorate and nitric acid [75]. Later, this approach was modified with a mixture of sulfuric acid and nitric acid with potassium chlorate [76–77]. Hummers et al. developed an efficient method for graphite oxidation [78], which involves a mixture of sodium nitrate, potassium perman-

ganate, and concentrated sulfuric acid. These approached are presently used methods for the oxidation of graphite [79–82].

Graphite oxide sheets contain oxygen functional groups on both sides of the plane and around the edges [83]. These oxygen function groups include hydroxyl groups, epoxide groups and carboxyl groups, which make graphite oxide highly hydrophilic. Single-layer or few-layer graphite oxide can be easily obtained by ultrasonication of graphite oxide in water or other organic solvents such as ethanol. Both graphite oxide and GO are electrically insulating materials due to their disrupted sp^2 bonding networks. The electrical conductivity can be recovered if the Π network is restored. To restore graphene structure, one of the most important reactions of GO is its reduction. The products are generally called chemically rGO.

Reduction of graphite oxides can be achieved by using various chemical reductants such as hydrazine [84], dimethylhydrazine [85], hydroquinone [86] and $NaBH_4$ [87] and H_2 at high temperature [88]. For instance, graphite oxide films are directly reduced in hydrazine by Kaner et al. [84]. Graphite oxide films are dispersed directly into hydrazine. Bubbles rapidly form along the film surface due to the chemical reduction, which likely produces NO_2 and N_2 as byproducts. After several hours, no graphite oxide paper can be visually observed in the dispersion and bubbling subsides, indicating good dispersion and complete reduction, respectively (as shown in Fig. 9(b)).

Compared to graphene which produced by mechanical cleavage and CVD, the advantages of rGO prepared from chemical or thermal reduction of GO lie in mass production and solution processability. Recently, we demonstrate patterning of rGO using soft nanolithography method. GO is synthesized from natural graphite flakes using modified Hummers' method. High quality and large area rGO pattern can be made on solid or flexible substrates by a polydimethylsiloxane (PDMS) based imprinting procedure. Stripe and square shaped micropatterns of GO film

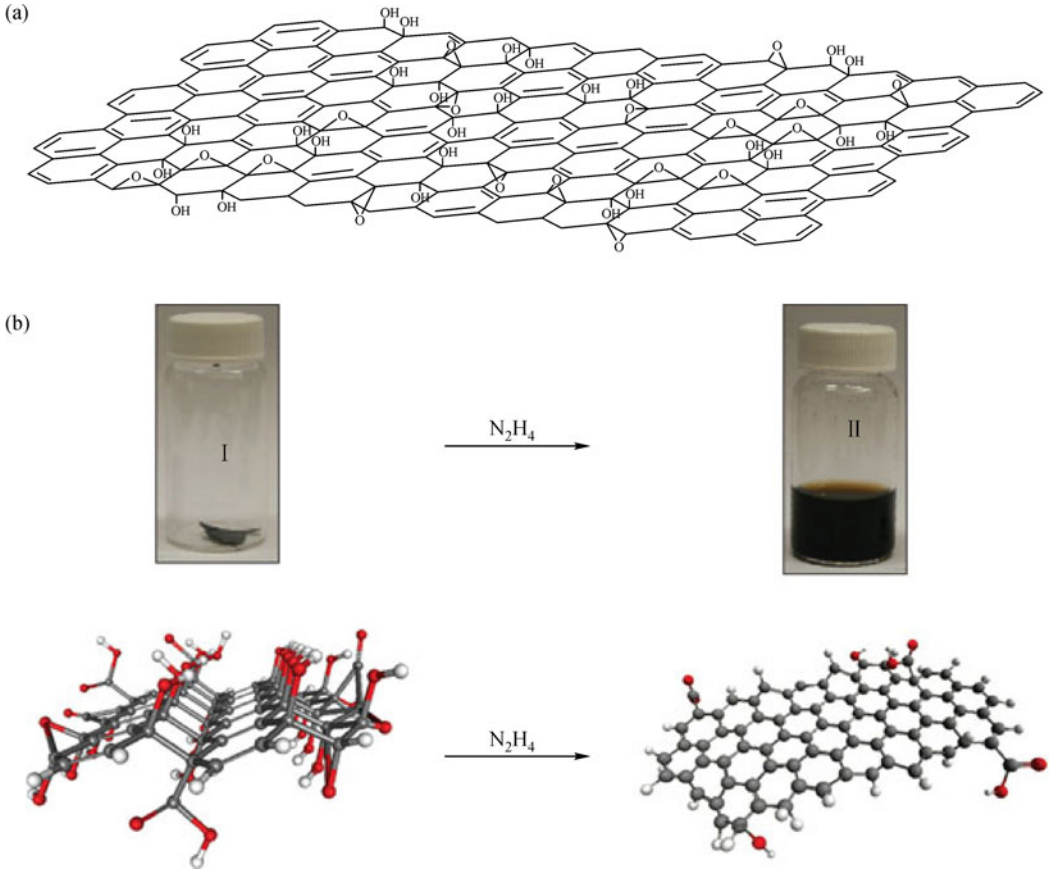

Fig. 9 **(a)** Model for as-prepared graphite oxide. (Reproduced with permission from Ref. [83], Copyright 1998 Elsevier) **(b)** Photographs of 15 mg of graphite oxide paper in a glass vial (I) and the resultant hydrazinium graphene (HG) dispersion after addition of hydrazine (II). Below each vial is a three-dimensional computer-generated molecular model of graphite oxide (carbon in grey, oxygen in red and hydrogen in white) and chemically converted graphene, respectively, suggesting that removal of –OH and –COOH functionalities upon reduction restores a planar structure. (Reproduced with permission from Ref. [84], Copyright 2009 Nature Publishing Group)

are generated from PDMS replication. Then the patterned GO films are reduced to rGO. As shown in Fig. 10, high quality stripe and square shaped rGO patterns are obtained; Further, array of rGO electronics are fabricated from the patterned film by a simple shadow mask method and gas sensors, which are based on these rGO electronics, show high sensitivity and recyclable usage in sensing NH_3 (as illustrated in Fig. 10(d)).

3.1.3 CVD

The most promising, low cost and readily accessible technique for growth of high quality and large area graphene is CVD, which has been receiving significant attention in recent years. In CVD, graphene grows from hydrocarbon gaseous species at high temperature in present of metallic thin film which both enhances the decomposition of hydrocarbon and nucleation of graphene lattice. The growth of layered graphene on transition metal surface has been known for 50 years. Layers of graphite were first observed on Ni surfaces that were exposed to carbon sources in the form of hydrocarbons or evaporated carbon [89]. Graphene growth has been demonstrated on a variety of transition metals including Ru [90], Ir [91], Co [92], Re [93], Ni [94] etc. via simple thermal decomposition of hydrocarbons on the surface or surface segregation of carbon upon cooling from a metastable carbon–metal solid solution. But breakthrough in preparation of large area graphene has been made by Kong et al. [94]. They exploited ambient pressure CVD on polycrystalline Ni films, to fabricate large area (~cm^2) films of single- to few-layer graphene and to transfer the films to nonspecific substrates. These films consist of regions of 1 to ~12 graphene layers. Single or bilayer regions can be up to

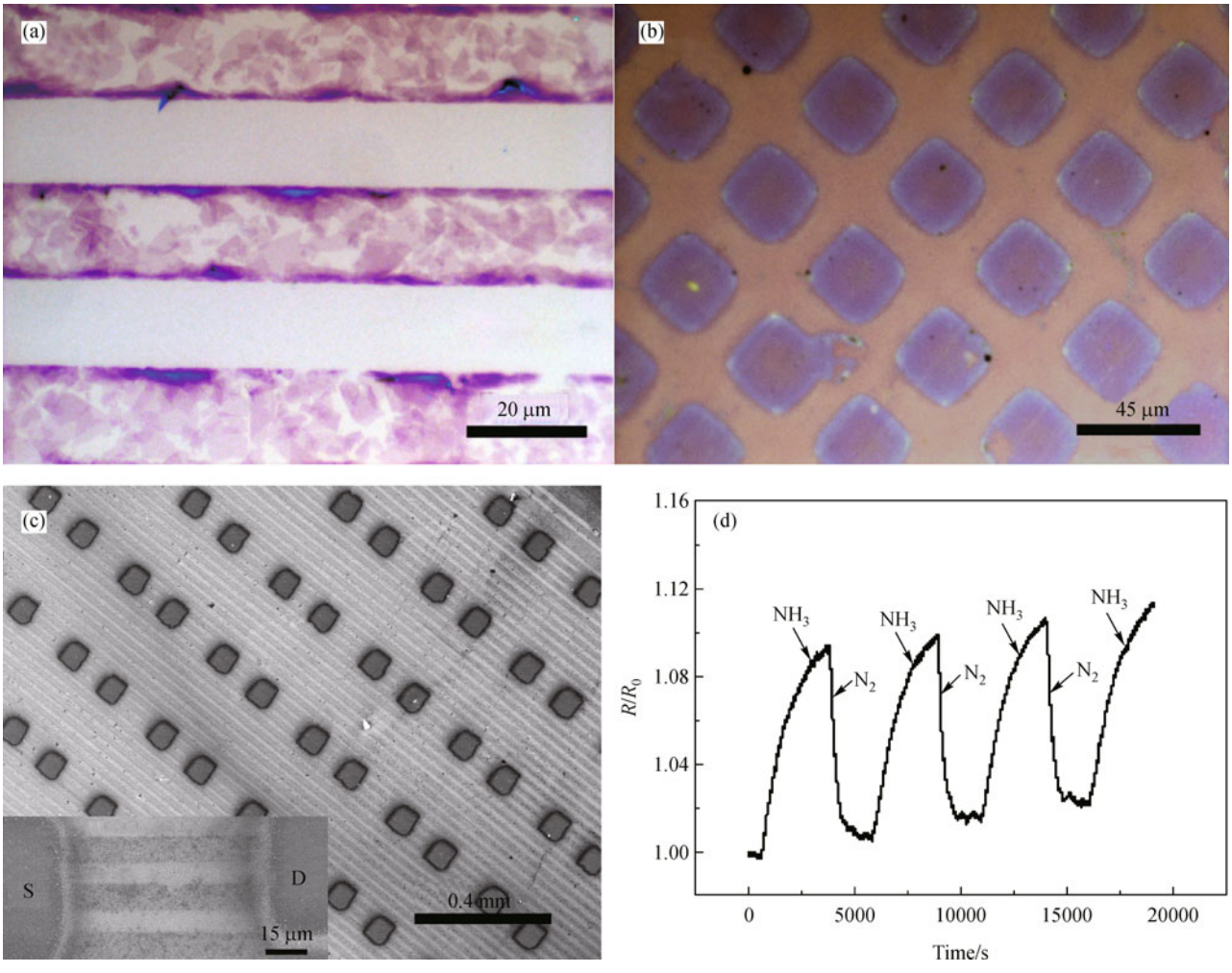

Fig. 10 Optical images of patterned rGO films: **(a)** striped shape; **(b)** square shape. **(c)** SEM image of the array of rGO TFT. Insert in (c) shows SEM image of a magnified device. **(d)** Adsorption and desorption of NH_3 on the rGO sensor. (Reproduced with permission from Ref. [88], Copyright 2011 Royal Society of Chemistry)

20 μm in lateral size. Further, Kim et al. demonstrated large scale patterned growth of graphene on patterned Ni film and transferring as grown graphene to arbitrary substrate [95]. This research presents great progress in the application of graphene for highly conducting and transparent electrodes in flexible, stretchable, foldable electronics. However, due to high solubility of carbon (0.258 wt.% at 1000°C), graphene prepared on nickel film exhibits small grain sizes and uncontrolled layered number, which limits its application. In contrast to nickel, high quality single-layer graphene over large areas has been achieved on copper foil recently by Ruoff et al. [96]. As shown in Fig. 11, the graphene grown on copper foil is predominantly single-layer graphene, with a small percentage (less than 5%) of the area having few layers, and are continuous across copper surface steps and grain boundaries. The formation of single-layer graphene on the copper is due to ultralow solubility of carbon in copper. Generally, the existence of numerous grains in film degrades the quality. To concern this problem, Ruoff et al. developed a two-step CVD process to synthesize graphene films with large single crystalline graphene [97]. The effect of growth parameters such as temperature, methane flow rate, partial pressure on the growth rate, domain size and surface coverage of graphene were studied systematically. Graphene domains having an area of hundreds of square micrometers can be achieved under optimized conditions. Yu et al. revealed that graphene grains show no definite epitaxial relationship with the copper substrate, and can cross copper grain boundaries [98]. And they further demonstrated an approach using pre-patterned growth seeds to control graphene nucleation and form graphene pattern on the substrate, which opened a route towards scalable fabrication of single-crystal graphene devices without grain boundaries.

Graphene growth is generally performed on metallic substrates, which are unsuitable for electrical devices and other applications. The grown graphenes have to be transferred to insulating substrate prior to device fabrication, which is technically demanding, time consuming and costly. To solve this problem, very recently, Liu et al. reported oxygen aided CVD was utilized to grow high-quality polycrystalline graphene directly on dielectric substrates [silicon dioxide (SiO_2) or quartz] without any metal film [99]. This method avoids the need for either a metal catalyst or a complicated and skilled post growth transfer process and is compatible with current silicon processing techniques. As shown in Fig. 12, the growth was carried out using a CVD system at atmospheric pressure. The growth substrates were activated in air to form nucleated sites at high temperature. Then high-quality polycrystalline graphene was subsequently grown on SiO_2 by utilizing the oxygen-based nucleation sites. Graphene modified SiO_2 substrates can be directly used in transparent conducting films and field-effect devices. The carrier mobilities are about 531 $cm^2 \cdot V^{-1} \cdot s^{-1}$ in air and 472 $cm^2 \cdot V^{-1} \cdot s^{-1}$ in N_2, which are close to that of metal-catalyzed polycrystalline graphene. Carbon sources for graphene growth in CVD are limited to gaseous carbon containing materials including methane, ethylene etc., which makes it difficult to apply the technology to a wider variety of potential feedstocks. Tour et al. demonstrated growth of graphene from solid carbon sources [100]. Large area and high quality graphene with controllable thickness can be grown from solid carbon sources such as polymer films or small molecules — deposited on a metal catalyst substrate at temperatures as low as 800°C. Both pristine graphene and doped graphene were grown with this one-step process.

3.2 Graphene electrical biosensor

Graphene is highly promising for the development of new types of chemical/biological sensors with ultrahigh sensitivity due to following reasons: 1) Graphene is a two-dimensional material and thus every atom can be exposed to the surface adsorbates, which maximizes the sensing effect [101]; 2) Graphene's highly conductive properties and few crystal can ensure a low level of excess (1/*f*) noise caused by thermal switching [102]; 3) The electronic properties of graphene are sensitive to both electron-donor and acceptor molecules, which renders graphene-based devices with high potential for sensing applications.

Recently, several reports demonstrated that graphene-based FETs with electrolyte top gating can be efficiently used as chemical/biological sensors. Das et al. have discussed monitoring dopants by Raman scattering in an electrochemically top-gated graphene-based FET [103]. They found that top gating graphene-based FETs was able to reach doping levels up to 5×10^{13} cm^{-2}. Such high doping level is possible because the Debye layer in the electrolyte gate provides much higher gate capacitance. Modulation of the conductance channel in solution-gated FETs can be achieved by applying a gate potential across the electrolyte, which acts as a dielectric. Because of the ambipolar characteristics of graphene, both hydroxyl

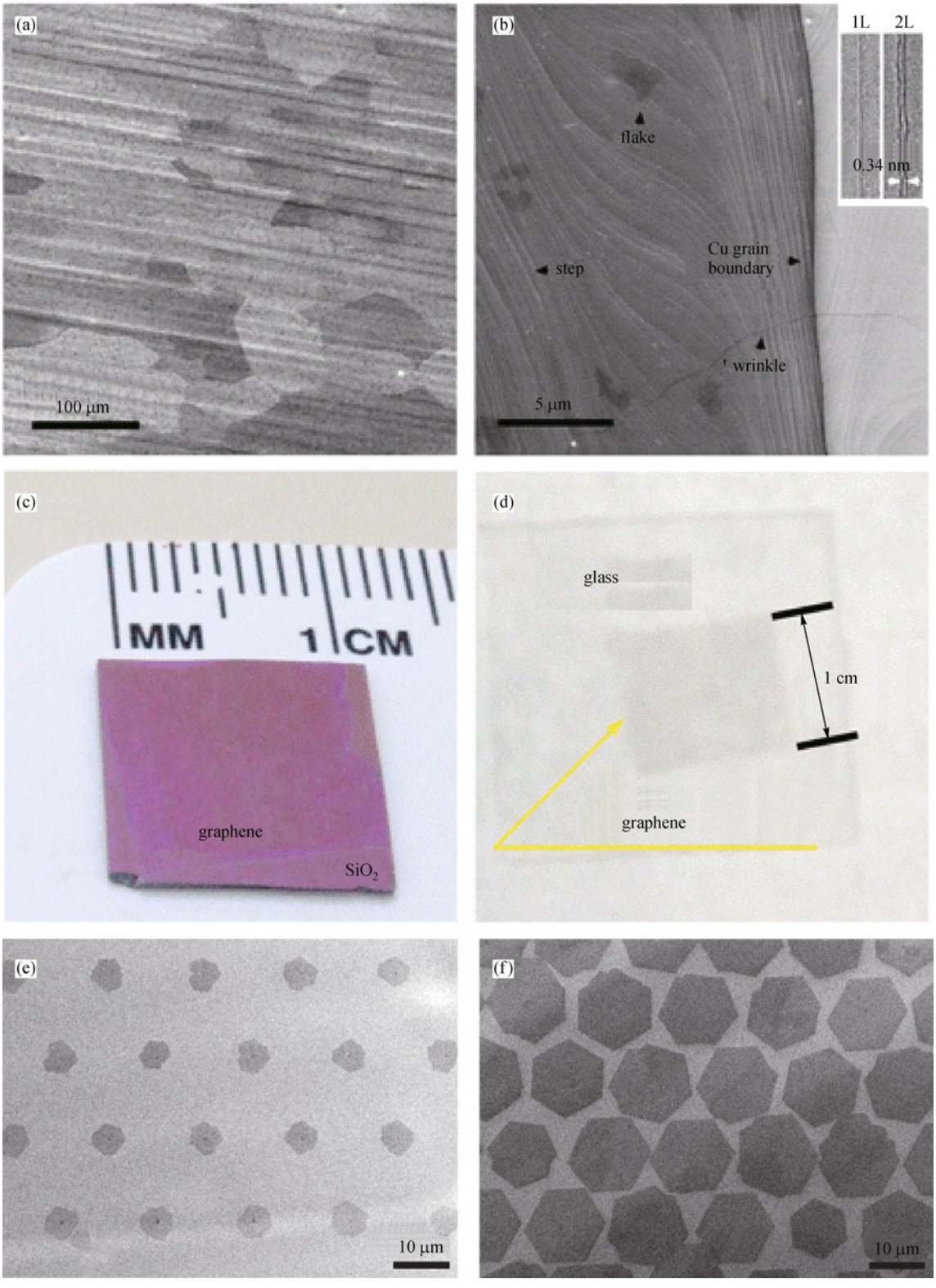

Fig. 11 **(a)** SEM image of graphene on a copper foil with a growth time of 30 min. **(b)** High-resolution SEM image showing a Cu grain boundary and steps, two- and three-layer graphene flakes, and graphene wrinkles. Inset in (b) shows TEM images of folded graphene edges. 1L, one layer; 2L, two layers. **(c)(d)** Graphene films transferred onto a SiO_2/Si substrate and a glass plate, respectively. (Reproduced with permission from Ref. [96], Copyright 2009 the American Association for the Advancement of Science) Graphene grown on the patterned seeds with the growth time of **(e)** 5 min and **(f)** 15 min. (Reproduced with permission from Ref. [98], Copyright 2011 Nature Publishing Group)

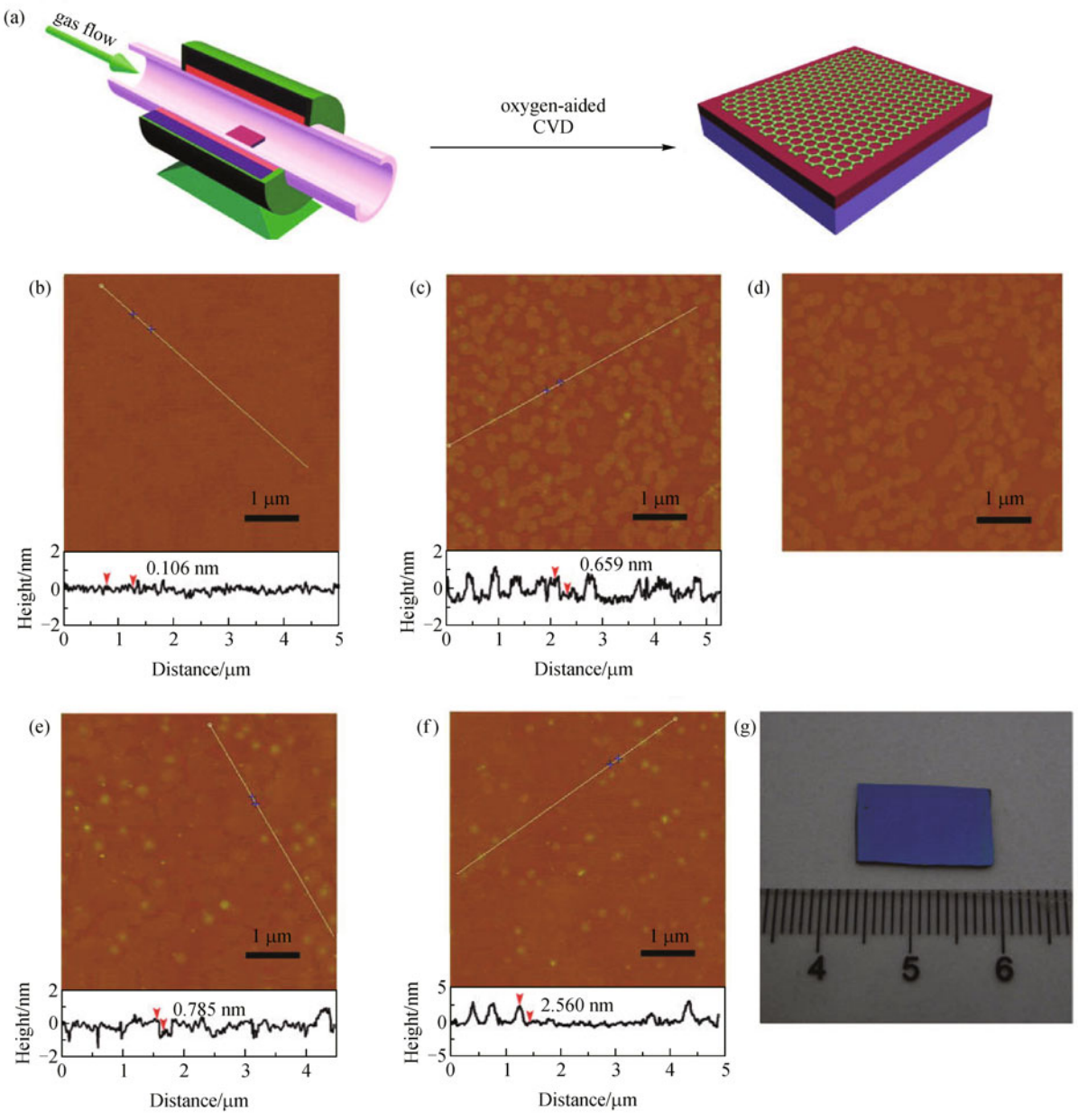

Fig. 12 **(a)** Schematic diagram of the oxygen-aided CVD growth of graphene on a SiO_2/Si substrate. **(b)** Initial surface of the SiO_2/Si substrate, characterized by a uniform flat surface. **(c)** AFM height image of graphene sheets with a thickness of ~0.659 nm. **(d)** AFM phase image of graphene sheets. **(e)** AFM image of two-dimensional interconnected graphene networks. **(f)** AFM image of continuous graphene films. **(g)** Photograph of a graphene film on SiO_2/Si substrate. The edge was removed using adhesive tape. (Reproduced with permission from Ref. [99], Copyright 2011 American Chemical Society)

(OH^-) and hydroxonium (H_3O^+) ions are proposed to be able to modulate the channel conductance of graphene-based FETs. Loh et al. demonstrated solution-gated epitaxial graphene as a pH sensor [104]. The sensor was fabricated from few-layer graphene epitaxially grown on an SiC substrate. The electrochemical double layer at the graphene/electrolyte interface is observed to be very sensitive to pH and the conductance of the device responded to pH changes.

Rao et al. studied the interaction of DNA nucleobases and nucleosides with graphene by isothermal titration calorimetry [105]. The results showed that the interaction energies of the nucleobases varies in the order guanine (G) > adenine (A) > cytosine (C) > thymine (T) in an aqueous solution. The same trend was found with the nucleosides. Interaction energies of A–T and G–C pairs are somewhere between those of the constituent bases. Theoretical calculations taking into account van der Waals interactions

and solvation energies suggest that the trend should be G > A > T > C. Recently, Ohno et al. demonstrated an electrolyte-gated graphene-based FET for detecting protein adsorption [106]. The graphene-based FET, which has a non-functionalized single-layer graphene as the channel, exhibited a linear increase in conductance upon the electrolyte pH – thus indicating its potential use in a pH sensor. Further investigation revealed that the conductance of the graphene-based FET increased with the adsorbed protein (bovine serum albumin) at a level of several hundred picomolar, which implied that the graphene-based FET can be used for highly sensitive electrical biosensors. Mohanty and Berry developed a graphene-based single bacterium resolution biodevice and DNA FET [107]. They first investigated the interaction between chemical modified graphene and bioentities. Chemical modified graphene and their biohybrids were synthesized from GO or plasma-modified graphene amine (GA). The DNA with a terminal amine group was bonded covalently with carboxylic group of GO by immersing GO coated silica in the amine DNA and amide coupling reagent O-(7-azabenzotriazole-1-yl)-N,N,N,N′-tetramethyluronium hexafluorophosphate (HATU) solution. This tethering was verified by hybridizing the DNA with a fluorescent cDNA probe. The Gram-positive Bacill cell with highly negatively charged surface was immobilized on GA via electrostatic interaction, which is measured by means of fluorescent microscopy. The electronic conductance of the bacterium device and the DNA transistor were investigated: the results showed that the bacteria biodevice was highly sensitive with a single-bacterium attachment generating ~1400 charge carriers in a p-type FET and DNA tethered on graphene hybridizes with its complementary DNA strand to reversibly increase the hole density by 5.61×10^{12} cm^{-2}. Dong et al. demonstrated that CVD-grown large-sized graphene films consisting monolayered and few-layered graphene domains were used to fabricate liquid gated transistors for DNA sensing applications [108]. The shift in $V_{g,min}$ of the probe DNA immobilized graphene transistors is found to be sensitive to addition of complementary DNA with a concentration as low as 0.01 nmol/L, due to electronic n-doping to the devices. Adding AuNPs on the surface of graphene devices can extend the upper limit of DNA detection (from 10 to 500 nmol/L) due to the increase in loading of the probe DNA molecules. Stine et al. demonstrated real-time, label-free detection of DNA hybridization using rGO FET devices [109]. The ease with which large area rGO films can be deposited and etched to form multiple devices enables us to incorporate reference sensors into our platform to mitigate the effects of non-specific biological interactions and improve specificity. The limit of detection for the rGO FETs compares favorably with other label-free detection platforms, and may offer a simple and low cost alternative to surface plasmon resonance (SPR) or nanowire devices.

4 Conclusions

Controlled growth of CNTs and graphene are essential for excellent electro-optical properties and application in electrical sensor. To realize the practical applications of CNTs in photoelectronic and chemical/biological device, great efforts have been made to control growth of CNTs and graphene with specific structures. Doping and aligned growth of CNTs by CVD present the two important strategies for application of CNTs in electronics. We have reviewed the latest research regarding this. Further, we present the latest progress in growth of graphene.

CNT-based FETs present promising strategies for future biological assay due to their ultrahigh sensitivity and potential for miniaturization. CNT-based FET sensors have been investigated for nearly ten years, and great progress has been achieved in the field. So far, most of the work has been focused on individual devices. To realize the practical applications of these promising analytic devices, future investigations should give emphasis to the development of arrays of CNT sensors. Issues concerning production methods, controlled modification of different individual devices with variable sensing materials, and other basic problems need to be resolved. Research on graphene-based FETs is still in its infancy but these devices have great promise in the fields of biological sensors. This new research field offers numerous challenges such as the development of simple reproducible fabrication methods and the understanding of the sensing mechanisms.

Acknowledgements This work was supported by the National Natural Science Foundation of China (Grant No. 61172001), the Scientific Research Foundation for the Returned Overseas Chinese Scholars, State Education Ministry, the Fundamental Research Funds for Central Universities, and Chinese Program for New Century Excellent Talents in University.

References

[1] Kroto H W, Heath J R, O'Brien S C, et al. C_{60}: Buckminsterfullerene. Nature, 1985, 318(6042): 162–163

[2] Iijima S. Helical microtubules of graphitic carbon. Nature, 1991, 354(6348): 56–58

[3] Novoselov K S, Geim A K, Morozov S V, et al. Electric field effect in atomically thin carbon films. Science, 2004, 306(5696): 666–669

[4] Jorio A, Dresselhaus G, Dresselhaus M S. Carbon Nanotubes: Advanced Topics in the Synthesis, Structure Properties and Applications. Berlin, Heidelberg: Springer-Verlag Berlin/Heidelberg, 2008

[5] de Heer W A, Chatelain A, Ugarte D. A carbon nanotube field-emission electron source. Science, 1995, 270(5239): 1179–1180

[6] Liu C, Fan Y Y, Liu M, et al. Hydrogen storage in single-walled carbon nanotubes at room temperature. Science, 1999, 286 (5442): 1127–1129

[7] Zandonella C. Is it all just a pipe dream? Nature, 2001, 410 (6830): 734–735

[8] Wu Z C, Chen Z H, Du X, et al. Transparent, conductive carbon nanotube films. Science, 2004, 305(5688): 1273–1276

[9] Zhang D H, Ryu K, Liu X L, et al. Transparent, conductive, and flexible carbon nanotube films and their application in organic light-emitting diodes. Nano Letters, 2006, 6(9): 1880–1886

[10] Zhang M, Fang S L, Zakhidov A A, et al. Strong, transparent, multifunctional, carbon nanotube sheets. Science, 2005, 309 (5738): 1215–1219

[11] Wei J Q, Zhu H W, Wu D H, et al. Carbon nanotube filaments in household light bulbs. Applied Physics Letters, 2004, 84(24): 4869–4871

[12] Pushparaj V L, Shaijumon M M, Kumar A, et al. Flexible energy storage devices based on nanocomposite paper. Proceeding of the National Academy of Sciences of the United States of America, 2007, 104(34): 13574–13577

[13] Kim S N, Rusling J F, Papadimitrakopoulos F. Carbon nanotubes for electronic and electrochemical detection of biomolecules. Advanced Materials, 2007, 19(20): 3214–3228

[14] Sugai T, Yoshida H, Shimada T, et al. New synthesis of high-quality double-walled carbon nanotubes by high-temperature pulsed arc dischargs. Nano Letters, 2003, 3(6): 769–773

[15] Montoro L A, Lofrano R C Z, Rosolen J M. Synthesis of single-walled and multi-walled carbon nanotubes by arc-water method. Carbon, 2005, 43(1): 200–203

[16] Bolshakov A P, Uglov S A, Saveliev A V, et al. A novel CW laser-power method of carbon single-wall nanotubes production. Diamond and Related Materials, 2002, 11(3–6): 927–930

[17] Zhang H Y, Ding Y, Wu C Y, et al. The effect of laser power on the formation of carbon nanotubes prepared in CO_2 continuous wave laser ablation at room temperature. Physica B: Condensed Matter, 2003, 325: 224–229

[18] Marchiori R, Braga W F, Mantelli M B H, et al. Analytical solution to predict laser ablation rate in a graphitic target. Journal of Materials Science, 2010, 45(6): 1495–1502

[19] Doorn S K, O'Connell M J, Zheng L X, et al. Raman spectral imaging of a carbon nanotube intramolecular junction. Physical Review Letters, 2005, 94(1): 016802 (4 pages)

[20] Piner R D, Zhu J, Xu F, et al. "Dip-Pen" nanolithography. Science, 1999, 283(5402): 661–663

[21] Lu J Q, Kopley T E, Moll N, et al. High-quality single-walled carbon nanotubes with small diameter, controlled density, and ordered locations using a polyferrocenylsilane block copolymer catalyst precursor. Chemistry of Materials, 2005, 17(9): 2227–2231

[22] Cubukcu E, Degirmenci F, Kocabas C, et al. Aligned carbon nanotubes as polarization-sensitive, molecular near-field detectors. Proceeding of the National Academy of Sciences of the United States of America, 2009, 106(8): 2495–2499

[23] Yao Y G, Li Q W, Zhang J, et al. Temperature-mediated growth of single-walled carbon-nanotube intramolecular junctions. Nature Materials, 2007, 6(4): 283–286

[24] Hu P A, Xiao K, Liu Y Q, et al. Multiwall nanotubes with intramolecular junctions (CN_x/C): Preparation, rectification, logic gates, and application. Applied Physics Letters, 2004, 84 (24): 4932–4935

[25] Wei D C, Liu Y Q, Cao L C, et al. A new method to synthesize complicated multi-branched carbon nanotubes with controlled architecture and composition. Nano Letters, 2006, 6(2): 186–192

[26] Wei D C, Cao L C, Fu L, et al. A new technique for controllably producing branched or encapsulating nanostructures in a vapor–liquid–solid process. Advanced Materials, 2007, 19(3): 386–390

[27] Ma Y F, Wang B, Wu Y P, et al. The production of horizontally aligned single-walled carbon nanotubes. Carbon, 2011, 49(13): 4098–4110

[28] Ding L, Tselev A, Wang J, et al. Selective growth of well-aligned semiconducting single-walled carbon nanotubes. Nano Letters, 2009, 9(2): 800–805

[29] Ishigami N, Ago H, Imamoto K, et al. Crystal plane dependent growth of aligned single-walled carbon nanotubes on sapphire. Journal of the American Chemical Society, 2008, 130(30): 9918–9924

[30] Jin Z, Chu H B, Wang J Y, et al. Ultralow feeding gas flow guiding growth of large-scale horizontally aligned single-walled carbon nanotube arrays. Nano Letters, 2007, 7(7): 2073–2079

[31] Huang S M, Cai X Y, Liu J. Growth of millimeter-long and horizontally aligned single-walled carbon nanotubes on flat substrates. Journal of the American Chemical Society, 2003, 125 (19): 5636–5637

[32] Hong B H, Lee J Y, Beetz T, et al. Quasi-continuous growth of ultralong carbon nanotube arrays. Journal of the American

Chemical Society, 2005, 127(44): 15336–15337

[33] Giepmans B N G, Adams S R, Ellisman M H, et al. The fluorescent toolbox for assessing protein location and function. Science, 2006, 312(5771): 217–224

[34] Weijer C J. Visualizing signals moving in cells. Science, 2003, 300(5616): 96–100

[35] Pease A C, Solas D, Sullivan E J, et al. Light-generated oligonucleotide arrays for rapid DNA sequence analysis. Proceeding of the National Academy of Sciences of the United States of America, 1994, 91(11): 5022–5026

[36] Huang C C, Chang H T. Selective gold-nanoparticle-based "turn-on" fluorescent sensors for detection of mercury(II) in aqueous solution. Analytical Chemistry, 2006, 78(24): 8332–8338

[37] Herr J K, Smith J E, Medley C D, et al. Aptamer-conjugated nanoparticles for selective collection and detection of cancer cells. Analytical Chemistry, 2006, 78(9): 2918–2924

[38] Gerion D, Chen F, Kannan B, et al. Room-temperature single-nucleotide polymorphism and multiallele DNA detection using fluorescent nanocrystals and microarrays. Analytical Chemistry, 2003, 75(18): 4766–4772

[39] Charlier J-C, Blase X, Roche S. Electronic and transport properties of nanotubes. Reviews of Modern Physics, 2007, 79 (2): 677–732

[40] Shim M, Javey A, Shi Kam N W, et al. Polymer functionalization for air-stable n-type carbon nanotube field-effect transistors. Journal of the American Chemical Society, 2001, 123(46): 11512–11513

[41] Chen R J, Bangsaruntip S, Drouvalakis K A, et al. Noncovalent functionalization of carbon nanotubes for highly specific electronic biosensors. Proceeding of the National Academy of Sciences of the United States of America, 2003, 100(9): 4984–4989

[42] Ajayan P M. Nanotubes from carbon. Chemical Reviews, 1999, 99(7): 1787–1800

[43] Zheng M, Jagota A, Semke E D, et al. DNA-assisted dispersion and separation of carbon nanotubes. Nature Materials, 2003, 2 (5): 338–342

[44] Williams K A, Veenhuizen P T M, de la Torre B G, et al. Nanotechnology: carbon nanotubes with DNA recognition. Nature, 2002, 420(6917): 761–763

[45] Star A, Tu E, Niemann J, et al. Label-free detection of DNA hybridization using carbon nanotube network field-effect transistors. Proceeding of the National Academy of Sciences of the United States of America, 2006, 103(4): 921–926

[46] Gui E, Li L, Lee P S, et al. Electrical detection of hybridization and threading intercalation of deoxyribonucleic acid using carbon nanotube network field-effect transistors. Applied Physics Letters, 2006, 89(23): 232104 (3 pages)

[47] Gui E L, Li L J, Zhang K, et al. DNA sensing by field-effect transistors based on networks of carbon nanotubes. Journal of the American Chemical Society, 2007, 129(46): 14427–14432

[48] Dong X, Lau C M, Lohani A, et al. Electrical detection of femtomolar DNA via gold-nanoparticle enhancement in carbon-nanotube-network field-effect transistors. Advanced Materials, 2008, 20(12): 2389–2393

[49] Martínez M T, Tseng Y C, Ormategui N, et al. Label-free DNA biosensors based on functionalized carbon nanotube field effect transistors. Nano Letters, 2009, 9(2): 530–536

[50] Dastagir T, Forzani E S, Zhang R, et al. Electrical detection of hepatitis C virus RNA on single wall carbon nanotube-field effect transistors. Analyst, 2007, 132(8): 738–740

[51] Balavoine F, Schultz P, Richard C, et al. Helical crystallization of proteins on carbon nanotubes: a first step towards the development of new biosensors. Angewandte Chemie International Edition, 1999, 38(13–14): 1912–1915

[52] Kam N W S, Dai H. Carbon nanotubes as intracellular protein transporters: generality and biological functionality. Journal of the American Chemical Society, 2005, 127(16): 6021–6026

[53] Jiang K, Eitan A, Schadler L S, et al. Selective attachment of gold nanoparticles to nitrogen-doped carbon nanotubes. Nano Letters, 2003, 3(3): 275–277

[54] Niyogi S, Hamon M A, Hu H, et al. Chemistry of single-walled carbon nanotubes. Accounts of Chemical Research, 2002, 35 (12): 1105–1113

[55] Chen R J, Zhang Y, Wang D, et al. Noncovalent sidewall functionalization of single-walled carbon nanotubes for protein immobilization. Journal of the American Chemical Society, 2001, 123(16): 3838–3839

[56] Holmlin R E, Chen X, Chapman R G, et al. Zwitterionic SAMs that resist nonspecific adsorption of protein from aqueous buffer. Langmuir, 2001, 17(9): 2841–2850

[57] Besteman K, Lee J-O, Wiertz F G M, et al. Enzyme-coated carbon nanotubes as single-molecule biosensors. Nano Letters, 2003, 3(6): 727–730

[58] Hu P A, Fasoli A, Park J, et al. Self-assembled nanotube field-effect transistors for label-free protein biosensors. Journal of Applied Physics, 2008, 104(7): 074310 (5 pages)

[59] Star A, Gabriel J-C P, Bradley K, et al. Electronic detection of specific protein binding using nanotube FET devices. Nano Letters, 2003, 3(4): 459–463

[60] Boussaad S, Tao N J, Zhang R, et al. *In situ* detection of cytochrome c adsorption with single walled carbon nanotube device. Chemical Communications, 2003, (13): 1502–1503

[61] Artyukhin A B, Stadermann M, Friddle R W, et al. Controlled electrostatic gating of carbon nanotube FET devices. Nano Letters, 2006, 6(9): 2080–2085

[62] Gui E L, Li L J, Zhang K, et al. DNA sensing by field-effect transistors based on networks of carbon nanotubes. Journal of the American Chemical Society, 2007, 129(46): 14427–14432

[63] Chen R J, Choi H C, Bangsaruntip S, et al. An investigation of the mechanisms of electronic sensing of protein adsorption on carbon nanotube devices. Journal of the American Chemical Society, 2004, 126(5): 1563–1568

[64] Byon H R, Choi H C. Network single-walled carbon nanotube-field effect transistors (SWNT-FETs) with increased Schottky contact area for highly sensitive biosensor applications. Journal of the American Chemical Society, 2006, 128(7): 2188–2189

[65] Tang X, Bansaruntip S, Nakayama N, et al. Carbon nanotube DNA sensor and sensing mechanism. Nano Letters, 2006, 6(8): 1632–1636

[66] Hecht D S, Ramirez R J A, Briman M, et al. Bioinspired detection of light using a porphyrin-sensitized single-wall nanotube field effect transistor. Nano Letters, 2006, 6(9): 2031–2036

[67] Heller I, Janssens A M, Männik J, et al. Identifying the mechanism of biosensing with carbon nanotube transistors. Nano Letters, 2008, 8(2): 591–595

[68] Geim A K, Novoselov K S. The rise of graphene. Nature Materials, 2007, 6(3): 183–191

[69] Berger C, Song Z, Li X, et al. Electronic confinement and coherence in patterned epitaxial graphene. Science, 2006, 312 (5777): 1191–1196

[70] Emtsev K V, Bostwick A, Horn K, et al. Towards wafer-size graphene layers by atmospheric pressure graphitization of silicon carbide. Nature Materials, 2009, 8(3): 203–207

[71] Sutter P W, Flege J I, Sutter E A. Epitaxial graphene on ruthenium. Nature Materials, 2008, 7(5): 406–411

[72] Robinson J T, Perkins F K, Snow E S, et al. Reduced graphene oxide molecular sensors. Nano Letters, 2008, 8(10): 3137–3140

[73] Lu C H, Yang H H, Zhu C L, et al. A graphene platform for sensing biomolecules. Angewandte Chemie International Edition, 2009, 48(26): 4785–4787

[74] Ohno Y, Maehashi K, Matsumoto K. Label-free biosensors based on aptamer-modified graphene field-effect transistors. Journal of the American Chemical Society, 2010, 132(51): 18012–18013

[75] Brodie B C. On the atomic weight of graphite. Philosophical Transactions of the Royal Society of London, 1859, 149: 249–259

[76] Staudenmaier L. Verfahren zur darstellung der graphitsaure. Berichte der Deutschen Chemischen Gesellschaft, 1898, 31(2): 1481–1487 (in German)

[77] Hamdi H. Zur Kenntnis der kolloidchemischen Eigenschaften des Humus Dispersoidchemische Beobachtungenan Graphitoxyd. Fortschrittsberichte uber Kolloide und Polymere, 1943, 54(10–12): 554–634 (in German)

[78] Hummers W S, Offeman R E. Preparation of graphitic oxide. Journal of the American Chemical Society, 1958, 80(6): 1339–1339

[79] Niyogi S, Bekyarova E, Itkis M E, et al. Solution properties of graphite and graphene. Journal of the American Chemical Society, 2006, 128(24): 7720–7721

[80] Hirata M, Gotou T, Horiuchi S, et al. Thin-film particles of graphite oxide: high-yield synthesis and flexibility of the particles. Carbon, 2004, 42(14): 2929–2937

[81] Kovtyukhova N I, Ollivier P J, Martin B R, et al. Layer-by-layer assembly of ultrathin composite films from micron-sized graphite oxide sheets and polycations. Chemistry of Materials, 1999, 11 (3): 771–778

[82] Lu J, Yang J X, Wang J, et al. One-pot synthesis of fluorescent carbon nanoribbons, nanoparticles, and graphene by the exfoliation of graphite in ionic liquids. ACS Nano, 2009, 3(8): 2367–2375

[83] He H, Klinowski J, Forster M, et al. A new structural model for graphite oxide. Chemical Physics Letters, 1998, 287(1–2): 53–56

[84] Tung V C, Allen M J, Yang Y, et al. High-throughput solution processing of large-scale graphene. Nature Nanotechnology, 2009, 4(1): 25–29

[85] Stankovich S, Dikin D A, Dommett G H B, et al. Graphene-based composite materials. Nature, 2006, 442(7100): 282–286

[86] Wang G, Yang J, Park J, et al. Facile synthesis and characterization of graphene nanosheets. Journal of Physical Chemistry C, 2008, 112(22): 8192–8195

[87] Si Y, Samulski E T. Synthesis of water soluble graphene. Nano Letters, 2008, 8(6): 1679–1682

[88] Zhang J, Hu P A, Zhang R F, et al. Soft-lithographic processed soluble micropatterns of reduced graphene oxide for wafer-scale thin film transistors and gas sensors. Journal of Materials Chemistry, 2012, 22(2): 714–718

[89] Banerjee B C, Hirt T J, Walker P L. Pyrolytic carbon formation from carbon suboxide. Nature, 1961, 192(4801): 450–451

[90] Himpsel F J, Christmann K, Heimann P, et al. Adsorbate band dispersions for C on Ru(0001). Surface Science Letters, 1982, 115(3): L159–L164

[91] Kholin A, Rut'kov E V, Tontegode A Y. Soviet Physics - Solid State, 1985, 27: 155

[92] Hamilton J C, Blakely J M. Carbon segregation to single crystal surfaces of Pt, Pd and Co. Surface Science, 1980, 91(1): 199–217

[93] Gall N R, Mikhallov S N, Rut'kov E V, et al. Soviet Physics - Solid State, 1985, 27: 1410

[94] Reina A, Jia X T, Ho J, et al. Large area, few-layer graphene films on arbitrary substrates by chemical vapor deposition. Nano

Letters, 2009, 9(1): 30–35

[95] Kim K S, Zhao Y, Jang H, et al. Large-scale pattern growth of graphene films for stretchable transparent electrodes. Nature, 2009, 457(7230): 706–710

[96] Li X S, Cai W W, An J H, et al. Large-area synthesis of high-quality and uniform graphene films on copper foils. Science, 2009, 324(5932): 1312–1314

[97] Li X S, Magnuson C W, Venugopal A, et al. Graphene films with large domain size by a two-step chemical vapor deposition process. Nano Letters, 2010, 10(11): 4328–4334

[98] Yu Q K, Jauregui L A, Wu W, et al. Control and characterization of individual grains and grain boundaries in graphene grown by chemical vapour deposition. Nature Materials, 2011, 10(6): 443–449

[99] Chen J Y, Wen Y G, Guo Y L, et al. Oxygen-aided synthesis of polycrystalline graphene on silicon dioxide substrates. Journal of the American Chemical Society, 2011, 133(44): 17548–17551

[100] Sun Z Z, Yan Z, Yao J, et al. Growth of graphene from solid carbon sources. Nature, 2010, 468(7323): 549–552

[101] Novoselov K S, Jiang D, Schedin F, et al. Two dimensional atomic crystals. Proceeding of the National Academy of Sciences of the United States of America, 2005, 102(30): 10451–10453

[102] Dresselhaus M S, Dresselhaus G. Intercalation compounds of graphite. Advances in Physics, 2002, 51(1): 1–186

[103] Das A, Pisana S, Chakraborty B, et al. Monitoring dopants by Raman scattering in an electrochemically top-gated graphene transistor. Nature Nanotechnology, 2008, 3(4): 210–215

[104] Ang P K, Chen W, Wee A T S, et al. Solution-gated epitaxial graphene as pH sensor. Journal of the American Chemical Society, 2008, 130(44): 14392–14393

[105] Varghese N, Mogera U, Govindaraj A, et al. Binding of DNA nucleobases and nucleosides with graphene. ChemPhysChem, 2009, 10(1): 206–210

[106] Ohno Y, Maehashi K, Yamashiro Y, et al. Electrolyte-gated graphene field-effect transistors for detecting pH and protein adsorption. Nano Letters, 2009, 9(9): 3318–3322

[107] Mohanty N, Berry V. Graphene-based single-bacterium resolution biodevice and DNA transistor: interfacing graphene derivatives with nanoscale and microscale biocomponents. Nano Letters, 2008, 8(12): 4469–4476

[108] Dong X C, Shi Y M, Huang W, et al. Electrical detection of DNA hybridization with single-base specificity using transistors based on CVD-grown graphene sheets. Advanced Materials, 2010, 22 (14): 1649–1653

[109] Stine R, Robinson J T, Sheehan P E, et al. Real-time DNA detection using reduced graphene oxide field effect transistors. Advanced Materials, 2010, 22(46): 5297–5300